

# Multi-Layer Control Architecture for the Reduction of Deterministic and Non-Deterministic Loads on Wind Turbines\*

C.L. Bottasso<sup>1†</sup>, A. Croce<sup>1</sup>, D. Devecchi<sup>1</sup>, C.E.D. Riboldi<sup>1</sup>, Y. Nam<sup>2</sup>

<sup>1</sup> Dipartimento di Ingegneria Aerospaziale, Politecnico di Milano, Milano, Italy

<sup>2</sup> Department of Mechanical and Mechatronics Engineering,  
Kangwon National University, Kangwon, Korea

**Keywords:** Wind turbine; variable speed regulation; pitch-torque control; individual blade pitch control; higher harmonic control; aero-servo-elasticity; multibody dynamics.

## Abstract

We describe a multi-layer architecture for the control of variable speed wind turbines, whereby each control layer targets a specific goal. The proposed architecture is inspired by the multi-objective nature of the wind turbine control problem.

Three main goals are identified and associated with three distinct control loops: a) trimming and load alleviation for large scale gusts engulfing the whole rotor disk, targeted by a collective-pitch/torque controller; b) alleviation of deterministic slowly varying and low frequency loads, targeted by a higher harmonic controller operating in the frequency domain; and c) alleviation of non-deterministic loads caused by small spatial and fast temporal wind fluctuation due to turbulence.

The proposed control architecture is demonstrated by means of various tests conducted in a high-fidelity simulation environment.

## Notation

$\alpha$	HHC relaxation factor
$\beta$	Blade pitch
$\psi$	Azimuth angle
$\rho$	Air density
$A$	Rotor area
$B$	Number of blades
$C_P$	Power coefficient
$J$	HHC cost function

---

\*Paper submitted to *Wind Energy*, under review, 2010. Paper presented at EWEA 2011, Bruxelles, Belgium, March 14–17, 2011.

<sup>†</sup>Corresponding author, Dipartimento di Ingegneria Aerospaziale, Politecnico di Milano, Via La Masa 34, Milano, 20156 Italy. E-mail: [carlo.bottasso@polimi.it](mailto:carlo.bottasso@polimi.it); Tel.: +39-02-2399-8315; Fax: +39-02-2399-8334.

$K$	Azimuthal sampling index
$k$	Measurement sampling index
$N_H$	Number of harmonics
$N_R$	Number of revolutions for signal demodulation
$N_T$	Number of trims for wind scheduling
$P$	Power
$R$	Rotor radius
$T$	Torque
$t$	Time
$V$	Wind speed
$\mathbf{b}$	Augmented vector of input harmonics
$\mathbf{I}$	Identity matrix
$\mathbf{s}$	Vector of harmonic bases
$\mathbf{T}$	Augmented transfer function
$\mathbf{u}$	Wind turbine control input vector
$\mathbf{z}$	Vector of output harmonics
$\mathbf{z}_0$	Vector of baseline output harmonics
$\Theta$	Jacobian of HHC outputs wrt inputs
$(\cdot)^T$	Transpose
$(\cdot)^{i,c}$	$i$ th cosine harmonic
$(\cdot)^{i,s}$	$i$ th sine harmonic
$(\cdot)_b$	Quantity pertaining to blade $b$
$(\cdot)_K$	Quantity referred to azimuthal sampling step $K$
$(\cdot)_k$	Quantity referred to sampling time step $t_k$
$(\cdot)_r$	Rated quantity, i.e. corresponding to the achievement of rated power
$(\cdot)_{\text{DEL}}$	Damage equivalent load
$(\cdot)_{\text{EXP}}$	Expected quantity
$(\cdot)_{\text{HHC}}$	Quantity referred to deterministic load-reducing control loop
$(\cdot)_{\text{ND}}$	Quantity referred to non-deterministic load-reducing control loop
$(\cdot)_{\text{ND}}$	Quantity referred to inner trimming loop
$(\cdot)$	Measured quantity

## 1 Introduction

In recent years several research activities have been focused on individual blade pitch control as a mean for reducing loads on crucial structural components of modern wind turbines, as blades, drive-train, bearings and tower. The current literature describes a variety of architectures of the control system and of approaches used for the synthesis of control laws, frequently using individual, decentralized or cyclic blade pitch control. For example, Refs. [1, 2, 3, 4] document the development of individual blade pitch control techniques based on the Coleman transform, later extended to higher harmonics in Ref. [5]. Reference [6] reports a similar approach, where the load alleviating control on each blade is implemented based on a decentralized architecture, superimposed to a baseline collective controller used for trimming the machine around each given set point. A decoupled approach is presented also in Ref. [7], where a pitch controller is used for reducing the 1P fluctuations of each blade root bending moment through a  $H_\infty$  approach. The effectiveness of a decentralized control architecture aimed at blade load reduction at frequencies that are multiple of rev has also been demonstrated in Ref. [8], while Ref. [9] has

studied a multivariable approach aimed at the synthesis of a time-domain controller capable of both trimming the machine and simultaneously reducing fatigue loads.

The present work fits within this active research area, and explores the multi-layer control architecture depicted in Fig. 1.

The proposed approach is based on a multi-layer architecture, inspired by the fact that the control of wind turbines is in general a multi-objective optimization problem with (often contrasting) goals characterized by different underlying physical phenomena and space-time scales. To address this issue, in the present approach each control layer aims at a specific control target and cooperates with the other layers towards the obtainment of the various control goals; this way, the choice of the controller used on each layer can be optimized and tailored to the specific control goal of that layer, thereby improving performance and simplifying tuning.

The multi-layer concept is here demonstrated with an implementation consisting of three main loops.

## 1.1 Inner Loop

The inner loop is responsible for the trimming of the machine, i.e. the regulation around a set point during power curve tracking, and for gust load alleviation. Typically, this control layer can be implemented as a collective-pitch/torque controller, using a primarily constant pitch – variable torque control logic in region II, a primarily variable pitch – constant torque logic in region III, and some coupled strategy in the transition region between the two [10]. The inner control loop is usually quite effective in the containment of loads caused by gusts characterized by a significant change of the wind speed over the entire rotor disk, where one needs a rapid collective change in pitch setting, possibly accompanied by a corresponding torque adjustment.

While a well designed and tuned collective-pitch/torque controller can perform very well in such cases, as witnessed by its widespread adoption by industry, such solution is not as effective in the reduction of the deterministic and non-deterministic load fluctuations that are responsible for the accumulation of fatigue damage to the structure, which require cyclic or individual blade pitch actuation.

## 1.2 Middle Loop

In the present control design, a middle loop (see Fig. 1) is responsible for the reduction of the deterministic loads; these are primarily caused by the blade weight and by the non-uniformity of the spatial distribution of the wind over the rotor disk. The latter effect is due to the vertical wind shear, possible lateral shear, and tower shadow effect, and to the fact that the wind direction is in general not parallel to the rotor axis, because of the rotor up-tilt and of the possible presence of lateral and vertical wind components (respectively due to operation in yawed conditions and to the terrain orography in proximity of the wind turbine). These loads in the rotating frame have a limited bandwidth, with their principal components located at the lower per rev harmonics (1P, 2P, 3P, etc.) and lower blade natural frequencies. The harmonic amplitudes of such loads change with rather slow characteristic times, of the order of a rotor revolution, following changes in rotor RPM due to changes in the mean wind speed.

In this work, a Higher Harmonic Control (HHC) law is used for the middle deterministic load layer. HHC is an optimal controller denoted by a quadratic cost function and formulated in the frequency domain, that uses a linear model to relate the harmonics of the inputs to those of the outputs (cfr. Refs. [12, 13, 14, 15] and references therein).

Two different implementations are described herein:

- a) When targeting blade loads, we use a *decentralized* controller operating the pitch of each single blade *individually*;
- b) When targeting loads in the fixed reference frame (e.g. on the shaft bearing, yaw bearing, tower root, or when targeting the air gap in a direct drive machine, etc.), we use a *centralized* implementation that results in the *coordinated* control of the rotor blades.

Since fatigue might be a design driver on some components of a machine and not on another, the choice of the centralized or decentralized implementation should reflect the specific characteristics of the target wind turbine.

### 1.3 Outer Loop

In principle, it would be possible to include in the HHC design a large number of harmonics, so as to make it effective in controlling also the quickly varying load components. However, this would make the problem of identifying the HHC input-output model much harder to solve. Hence, the HHC design used here accounts only for the slower harmonics dominating the deterministic response, while the control architecture includes also an additional outer control loop (see Fig. 1) targeting non-deterministic blade loads. These are defined as those loads which are caused by variations of the wind with fast temporal scales (fractions of a rotor revolution) and/or small spatial scales (small azimuthal angles, experienced by a blade in a fraction of a revolution), which are typical of wind turbulence.

In this work the outer loop is implemented as follows:

- a) In the *decentralized* case, a simple PD controller operates individually on each single blade, driven by estimates of the non-deterministic blade loads, computed as differences of the total measured loads and the lower harmonic ones feeding the middle control layer (cfr. the cross-feed link connecting the inner and outer loops in Fig. 1 and see §2.2.1 for details);
- b) In the *centralized* case, the simple but very effective Coleman-transform proportional-integral individual-blade-pitch (IPC) algorithm of Ref. [1] is used.

In general, little can be said about the stability of a multi-loop architecture as the one used here. However, the individual blade pitch amplitudes commanded by the middle and outer loops are typically limited to rather small values for a number of reasons, as for example not to affect the regulation at the set point, to limit the actuator duty cycle, and to avoid excessive pitch differences among the blades that might lead to large loads in the case of extreme gusts. As such, these small individual pitch changes can be treated as disturbances, and the overall stability of the system will be determined to a large extent by the robustness to uncertainty of the underlying collective pitch controller, which is typically quite good.

## 2 Formulation of the Controller

The pitch-torque input vector to the wind turbine is  $\mathbf{u} = (\dots, \beta_b, \dots, T)$ , where  $\beta_b$  is the blade pitch input for the  $b$ th blade,  $b = (1, B)$ , and  $B$  is the number of blades, while  $T$  is the commanded generator torque. According to the control architecture of Fig. 1, input  $\mathbf{u}$  is obtained as the sum of the contributions of the various control layers as

$$\mathbf{u} = \mathbf{u}_T + \mathbf{u}_{\text{HHC}} + \mathbf{u}_{\text{ND}}, \quad (1)$$

where  $\mathbf{u}_T = (\dots, \beta_{b_T}, \dots, T_T)$  is the pitch-torque input provided by the inner trimmer (subscript  $(\cdot)_T$ ), with  $\beta_{1_T} = \dots = \beta_{B_T}$  if this is a collective controller,  $\mathbf{u}_{\text{HHC}} = (\dots, \beta_{b_{\text{HHC}}}, \dots, 0)$  the input provided by the middle deterministic load-reducing higher harmonic controller (subscript  $(\cdot)_{\text{HHC}}$ ), and  $\mathbf{u}_{\text{ND}} = (\dots, \beta_{b_{\text{ND}}}, \dots, 0)$  the pitch input provided by the outer non-deterministic (subscript  $(\cdot)_{\text{ND}}$ ) load-reducing loop.

## 2.1 Deterministic Loads: Formulation of the HHC Control Loop

In this work, the middle layer is implemented using the HHC approach (cfr. Ref. [12] for details and background information). The algorithm consists of four main steps: 1) demodulation from the time to the frequency domain of inputs and outputs (respectively, blade pitch and target loads); 2) identification of a linear model relating harmonics of the inputs to those of the outputs; 3) calculation of the inputs by solving an optimal control problem; 4) remodulation of the computed optimal input harmonics, to obtain the time domain inputs. Details regarding the implementation of these steps are given in the following.

### 2.1.1 Signal Demodulation

The signal demodulation problem is here formulated as described next, specifically accounting for the fact that wind turbines operate at variable rotor speed. At the rotor azimuthal position  $\psi_K = K\Delta\psi$ , one wants to demodulate a signal  $a(t)$  that is available in terms of measurements  $\hat{a}(t_k)$ , sampled at times  $t_k = k\Delta t$ , over the previous  $N_R$  revolutions (typically,  $N_R = 1$  here). Notice that there are two different sampling rates, one in space and the other one in time:

- A slow azimuthal sampling  $\Delta\psi$  corresponding to the frequency with which demodulation is performed (typically, four times per rev here), whose steps are indicated by index  $K$ . Notice that, on account of the fact that the rotor RPM on a wind turbine varies in time, a spatial sampling based on the rotor azimuth is used instead of a temporal sampling.
- A fast time sampling  $\Delta t$  corresponding to the measurement rate of the sensors (typically, in the range of the tens of Hz), whose steps are labeled by index  $k$ .

Demodulation of the signal over a window of  $N_R$  revs is expressed as

$$\hat{a}(t_k) = \hat{a}(\psi(t_k)) \approx \mathbf{a}_K^T \mathbf{s}(\psi(t_k)), \quad \psi(t_k) \in [\psi_K - 2\pi N_R, \psi_K], \quad (2)$$

where  $\mathbf{a}_K = (a_K^0, \dots, a_K^{i,s}, a_K^{i,c}, \dots)^T$  is the unknown vector of harmonic amplitudes at the current demodulation step  $K$ , and  $\mathbf{s}(\psi(t_k)) = (1, \dots, \sin(i\psi(t_k)), \cos(i\psi(t_k)), \dots)^T$ ,  $i = (1, N_H)$ , is the vector of  $N_H$  harmonic bases. The demodulation operation involves samples available at all time steps  $t_k$  covered during the last  $N_R$  revolutions. At the next demodulation step  $K + 1$ , corresponding to an increase in rotor azimuth of the angle  $\Delta\psi$ , the new samples gathered over the  $\Delta\psi$  rotation are added to the head of the demodulation window, while the oldest samples are discarded from its tail, to keep its azimuthal coverage of constant length.

The current estimate of the sine and cosine components of the  $i$ th harmonic amplitude, labeled respectively  $a_K^{i,s}$  and  $a_K^{i,c}$ , can be computed by projection as

$$a_K^{i,s} = \frac{1}{\pi N_R} \int_{\psi_K - 2\pi N_R}^{\psi_K} \hat{a}(\psi) \sin(i\psi) d\psi, \quad (3a)$$

$$a_K^{i,c} = \frac{1}{\pi N_R} \int_{\psi_K - 2\pi N_R}^{\psi_K} \hat{a}(\psi) \cos(i\psi) d\psi, \quad (3b)$$

where the integrals are approximated using the classic trapezoidal rule.

### 2.1.2 Model Identification

The input-output model takes the form [12]

$$\mathbf{z}_K = \mathbf{T}(V)\mathbf{b}_K, \quad (4)$$

where the vector of output harmonics is

$$\mathbf{z}_K = (\dots, z_K^{i,s}, z_K^{i,c}, \dots)^T, \quad (5)$$

the vector of HHC input harmonics is

$$\mathbf{b}_{\text{HHC}_K} = (\dots, \beta_K^{j,s}, \beta_K^{j,c}, \dots)^T, \quad (6)$$

and  $\mathbf{b}_K = (\mathbf{b}_{\text{HHC}_K}^T \mathbf{1})^T$  its augmented form. Matrix  $\mathbf{T}(V) = [\Theta(V)\mathbf{z}_0(V)]$  is the augmented transfer function, that includes the Jacobian  $\Theta(V)$  of the outputs with respect to the inputs, and the baseline output harmonics  $\mathbf{z}_0(V)$ , which account for the non-HHC related response of the machine. The notation highlights the fact that these quantities, in general, depend on the wind speed  $V$ , and hence Eq. (4) represents a linear parameter varying model.

In this work, input-output models are identified off-line. Since the model typically depends on the wind speed, separate identifications are conducted at a number of trim points of interest, that cover the entire operating range of wind speeds of the machine. At each trim point, denoted by the wind speed  $V_m$ ,  $m = (1, N_T)$ , model (4) is identified by subjecting the plant to a suitable excitation, recording the response of the machine, demodulating inputs and outputs, and finally estimating  $\mathbf{T}(V_m)$  using least-squares.

We consider an excitation phase lasting  $M$  rotor revolutions; over the  $K$ th revolution, inputs and outputs are demodulated as previously explained using (3) with  $\Delta\psi = 2\pi$ , which yields estimates of the harmonic amplitudes of the two signals. The input and output harmonics of interest, i.e. those that enter into the definition of the input-output model (4), are gathered in vectors  $\mathbf{z}_K$  and  $\mathbf{b}_{\text{HHC}_K}$ , respectively, and stored in matrices as

$$\mathbf{Z} = [\dots \mathbf{z}_K \dots], \quad (7a)$$

$$\mathbf{B} = [\dots \mathbf{b}_K \dots]. \quad (7b)$$

Minimization of the Frobenius norm  $\|\mathbf{E}\| = \sqrt{\sum_{ij} E_{ij}^2}$  of the model error matrix  $\mathbf{E} = \mathbf{Z} - \mathbf{T}(V_m)\mathbf{B}$ , yields the least-squares estimate of the augmented transfer function at the current trim point:

$$\mathbf{T}(V_m) = \arg \min_{\mathbf{T}(V_m)} \frac{1}{2} \|\mathbf{E}\|^2 = \mathbf{Z}\mathbf{B}^T(\mathbf{B}\mathbf{B}^T)^{-1}. \quad (8)$$

### 2.1.3 Control Law

The HHC control action is obtained by minimizing the cost

$$J = \frac{1}{2} (\mathbf{z}_K^T \mathbf{Q} \mathbf{z}_K + \Delta \mathbf{b}_{\text{HHC}_K}^T \mathbf{R} \Delta \mathbf{b}_{\text{HHC}_K}), \quad (9)$$

subjected to the input-output model constraint (4). The symmetric weight matrices  $\mathbf{Q}$  and  $\mathbf{R}$  may be scheduled as functions of the mean wind, i.e.  $\mathbf{Q} = \mathbf{Q}(V)$  and  $\mathbf{R} = \mathbf{R}(V)$ . Vector  $\Delta \mathbf{b}_{\text{HHC}_K}$  represents the increment to the HHC control input in the frequency domain between step  $K$  and step  $K + 1$ , i.e.

$$\mathbf{b}_{\text{HHC}_{K+1}} = \mathbf{b}_{\text{HHC}_K} + \alpha \Delta \mathbf{b}_{\text{HHC}_K}, \quad (10)$$

$\alpha \in [0, 1]$  being a relaxation factor used for controlling stability and quickness of the controller [14].

Imposing the stationarity of the cost augmented by the constraints with respect to the input increment, leads to the optimal control policy:

$$\Delta \mathbf{b}_{\text{HHC}_K} = -(\Theta(V)^T \mathbf{Q} \Theta(V) + \mathbf{R})^{-1} \Theta(V)^T \mathbf{Q} z_K, \quad (11)$$

which is driven by the demodulated blade loads at the current step,  $z_K$ .

Wind scheduling is obtained by estimating the current mean wind  $V$  by using a moving average over a window of about 10 seconds of the instantaneous turbulent samples provided by an anemometer or a wind observer [11]. The wind scheduled input-output model is obtained by linear interpolation of the values stored at the trim points  $t$  and  $t + 1$ , i.e.

$$\Theta(V) = (1 - \xi) \Theta(V_m) + \xi \Theta(V_{m+1}), \quad (12)$$

where  $\xi = (V - V_m)/(V_{m+1} - V_m)$ ,  $\xi \in [0, 1]$ .

The optimal HHC input (10) is held fixed until the next  $K$  step. At each one of the fast sampling time instants  $t_k$  at which the inner control loop operates, the HHC control input is modulated back in the time domain, added to the current input provided by the inner controller, and fed to the actuators.

The choice of the HHC control update frequency, i.e. the azimuthal spacing of the  $K$  steps, is related to the choice of the harmonics in the HHC controller, and one should use faster updates in connection with an increasing number of harmonics targeted by the controller. In the examples shown later in this work, the highest harmonic never exceeded the 7P, and it was found that  $K$  steps could be spaced apart of a quarter of a revolution. In fact, faster updates did not lead to improvements in the quality of the results, since enough new measurements are necessary to generate changes in the estimates of the harmonic amplitudes.

## 2.2 Decentralized and Centralized Implementations

### 2.2.1 Decentralized Architecture

In the decentralized control architecture, depicted in Fig. 2, each blade operates independently from the other ones under the action of its own controller. This arrangement is suitable when the aim is the reduction of the blade loads; notice that, since there is no coordination among the blades in this case, lower blade loads might not always imply similarly lowered loads in the fixed system (e.g., at the main or yaw bearings).

The HHC controllers are implemented as previously explained, using harmonics from 1P up to typically 3P both for inputs and outputs.

The external control loop is implemented as follows. Using the model definition (4), for a given wind speed  $V$  (which corresponds to a given input from the inner trimmer) and given control input  $\mathbf{b}_{\text{HHC}_K}$ , the harmonic amplitudes that one should expect to be observing on the blade are

$$z_{\text{EXP}_K} = z_0(V) + \Theta(V) \mathbf{b}_{\text{HHC}_K}. \quad (13)$$

This frequency domain load, modulated back in time using the vector of harmonic bases and evaluated at the current instant  $t_k$ , yields an expected load

$$z_{\text{EXP}}(t_k) = z_{\text{EXP}_K}^T \mathbf{s}(\psi(t_k)). \quad (14)$$

In the absence of turbulence, and clearly in the absence of modeling errors as well, this quantity should match the load measured by the load sensors at the current time instant.

Hence, any difference with respect to the value provided by Eq. (14) can be interpreted as a fast disturbance generated by turbulence, which should induce a feedback in the blade pitch so as to try to reject it. The difference between the current sensor reading  $\hat{z}(t_k)$ , low-pass filtered so as to damp the effect of noise, and the expected value is computed as

$$\Delta z(t_k) = \hat{z}(t_k) - z_{\text{EXP}}(t_k). \quad (15)$$

Based on this estimate of the load fluctuation, the pitch input of the non-deterministic layer is computed using a simple proportional-derivative control as

$$\beta_{\text{ND}}(t_k) = -K_P \Delta z(t_k) - K_D \frac{d\Delta z(t_k)}{dt}. \quad (16)$$

This additional pitch input is combined with the ones provided by the inner and middle layers according to Eq. (1), and sent to the blade actuators.

### 2.2.2 Centralized Architecture

The centralized control architecture is depicted in Fig. 3. This architecture is suitable when the aim is the reduction of the loads in the fixed system (e.g., at the main or yaw bearings). In fact, in contrast to the previous decentralized case, the action of the three blades must be coordinated to give a positive effect on one common target load.

A single centralized HHC controller is used for computing the pitch inputs of the master blade ( $b = 1$ ), while the other blades are commanded using a cyclic pitch regulation logic. The HHC input vector (Eq. (6)) is represented by the blade pitch harmonics of the master blade. The master blade pitch input in the time domain is computed as

$$\beta_1(t_k) = \beta_{1K}^T \mathbf{s}(\psi_1(t_k)), \quad (17)$$

where the vector of master blade pitch amplitudes is  $\beta_{1K} = (\dots, \beta_{1K}^{j,s}, \beta_{1K}^{j,c}, \dots)^T$ , and  $\mathbf{s}(\psi_1(t_k)) = (1, \dots, \sin(i\psi_1(t_k)), \cos(i\psi_1(t_k)), \dots)^T$  is its harmonic base vector, with  $i = (1, N_H)$ . The time-domain pitch of the other blades is readily obtained as

$$\beta_b(t_k) = \beta_{bK}^T \mathbf{s}(\psi_b(t_k)), \quad (18)$$

where  $\psi_b(t_k) = \psi_1(t_k) - 2\pi(b-1)/B$ ,  $b = (2, B)$ .

The HHC output vector (Eq. (5)) is represented by the harmonics of the moment components in the fixed system. If the machine is equipped with sensors that can measure the fixed system load components, then these quantities can be used directly; on the other hand, if the machine is equipped with sensors at the blade roots, then the fixed system components can be computed by using the Coleman transformation [1], as shown in Fig. 3.

The choice of harmonics of inputs and outputs must be made considering the filtering characteristics of a rotor [16]. For example, the shaft bending moment will contain mostly harmonics at the multiple of the number of blades,  $iBP$  (for example 3P, 6P, etc. for a three bladed rotor), and is affected by pitch inputs at  $i(B-1)P$  and  $i(B+1)P$  harmonics (for example, 2P and 4P blade pitch inputs control 3P loads).

The non-deterministic loop is implemented using the formulation of Ref. [1], where two independent single-input/single-output (SISO) proportional-integral (PI) controllers are used for reducing the d-q axis [1] loads, i.e. the fixed system yawing and nodding moment components.

If  $\hat{z}_d(t_k)$  and  $\hat{z}_q(t_k)$  are the two d-q measured load components at time  $t_k$ , the fixed system PI pitch inputs are defined as

$$\beta_d(t_k) = -K_P \hat{z}_d(t_k) - K_I \int_{t_k - T_I}^{t_k} \hat{z}_d(\tau) d\tau, \quad (19a)$$

$$\beta_q(t_k) = -K_P \hat{z}_q(t_k) - K_I \int_{t_k - T_I}^{t_k} \hat{z}_q(\tau) d\tau. \quad (19b)$$

The corresponding blade pitch inputs are computed using the partial inverse Coleman transform  $\mathbf{C}(t_k)$  as

$$\begin{Bmatrix} \beta_{ND_1}(t_k) \\ \beta_{ND_2}(t_k) \\ \beta_{ND_3}(t_k) \end{Bmatrix} = \mathbf{C}(t_k) \begin{Bmatrix} \beta_d(t_k) \\ \beta_q(t_k) \end{Bmatrix}, \quad (20)$$

where

$$\mathbf{C}(t_k) = \begin{bmatrix} \cos \psi_1(t_k) & \sin \psi_1(t_k) \\ \cos \psi_2(t_k) & \sin \psi_2(t_k) \\ \cos \psi_3(t_k) & \sin \psi_3(t_k) \end{bmatrix}. \quad (21)$$

These additional pitch inputs are combined with the ones provided by the inner and middle layers according to Eq. (1), and sent to the blade actuators.

### 3 Results

The example tests were conducted using a 2.5 MW class A wind turbine, having a rated wind speed  $V_r = 11$  m/s, a rotor radius  $R = 48$  m and a tower height  $H = 77$  m. The inner loop uses a PID feedback term on the collective blade pitch driven by the rotor angular speed error, while the input torque is tabulated as a function of the current RPM and requested pitch. The pitch actuators in the plant simulation are modeled as second order systems, with a maximum pitch rate of 7 deg/s. The machine is equipped with blade root strain gages, which provide the readings for the load alleviating middle and outer loops at 20 Hz; when needed, loads in the fixed system are computed by use of the Coleman transform [1].

All simulations were conducted using the software **Cp-Lambda** (Code for Performance, Loads and Aeroelasticity by Multi-Body Dynamic Analysis), based on a finite-element multibody formulation (see Ref. [17] and references therein).

#### 3.1 Quality Assessment of the Model Identification Phase

Input-output models were identified for both the centralized and decentralized implementations of the HHC controller. Pitch signals were obtained directly from the controller inputs sent to the actuators; this way, the identified model automatically takes into account the pitch actuator dynamics. The identification process was based on simulations performed in non-turbulent wind conditions, with hub speeds between 5 and 19 m/s. At each trim condition, the plant **Cp-Lambda** model was excited using a modulated pitch input featuring a prescribed harmonic content, for a duration of fifteen rotor revolutions. The pitch input was generated as a smooth signal with a different frequency content at each revolution, to improve the conditioning of the identification process. The response of the plant was used for identifying the input-output model, using the procedure described previously.

To verify the generality of the identification process, the plant **Cp-Lambda** and the identified models were excited with new pitch input time histories, having the same frequencies as those

used for identification but with different amplitudes and phases. As an example relative to the decentralized implementation, Fig. 4 shows the normalized time histories of the out-of-plane blade root bending moment generated by the plant and by the identified model during this new excitation phase. The model shows an excellent fidelity to the plant, both in terms of amplitude and of phase. Results of similar quality were obtained at other trim points.

## 3.2 Centralized Implementation

### 3.2.1 Load Reduction in Deterministic Wind

In the centralized case, the target load is chosen as the bending moment at the low speed shaft cross section located at the interface with the rotor hub. In steady wind conditions, this load oscillates at the triple multiples of the rev frequency (i.e. 3P, 6P, etc.). As a consequence, the HHC model was synthesized using the 3P and 6P harmonics of the outputs, and the 2P, 4P, 5P and 7P harmonics of the inputs.

After having identified models at a few trim points (specifically, every 4 m/s starting from 5 up to 25 m/s), as previously explained, simulations were carried out in constant-in-time winds, so as to perform a first assessment of the effectiveness of the proposed control architecture in the reduction of deterministic loads. The HHC load-reducing layer used diagonal weighting, tuned so as to achieve satisfactory load reduction performance without an excessive increase in pitch duty cycle. The HHC control law was updated four times per revolution, using the relaxation factor  $\alpha = 0.1$ .

Figure 5 shows the spectra of the normalized resultant of the shaft bending moment, for a constant wind speed of 15 m/s and an exponential shear layer coefficient of 0.2. Three control systems were considered here: the collective PID trimmer, the same PID trimmer coupled to the SISO PI IPC controller of Bossanyi [1] (termed in the following B-IPC), and the proposed controller (trimmer with centralized HHC and external B-IPC loop) shown in Fig. 3. In our implementation, we considered wind-scheduled gains for the B-IPC loop, to get an optimized performance with varying wind speed conditions.

As expected, the B-IPC controller nicely reduces the load mean value (cfr. the markers at the null frequency). B-IPC is also rather capable of reducing the 3P load harmonics, but its effect is very limited or even slightly negative at the higher multiples of rev. On the contrary, the addition of the HHC loop, while still taking advantage of the good qualities of B-IPC (in terms of reduction of the load mean value and 3P harmonic), effectively reduces also the higher harmonics of the target load.

### 3.2.2 Load Reduction in Turbulent Wind

Next, simulations were conducted in turbulent wind conditions of category A intensity for a duration of 600 s, for mean hub winds between 11 and 23 m/s. To account for some of the slower effects caused by turbulent fluctuations, an estimate of the mean wind was computed using a moving average of the anemometer reading using a time window of 10 s. The estimated mean wind speed was used for interpolating the models previously identified at the selected trim points.

A representation of the performance of the controllers is provided by the bar diagrams of Fig. 6. The figure refers to a mean hub wind speed of 21 m/s, and reports the percent change in Standard Deviation (STD) and Damage Equivalent Load (DEL) for the blade root and shaft bending moments, together with the percent change in STD and mean values of generated power.

DELs were computed by using rain-flow analysis as

$$M_{\text{DEL}} = \left( \sum_i \Delta M_i^m N_i / N_{\text{tot}} \right)^{1/m}, \quad (22)$$

$\Delta M_i$  being the  $i$ th cycle amplitude,  $N_i$  the number of cycles at the  $i$ th amplitude, and  $N_{\text{tot}}$  the total number of cycles. For the S-N fatigue slope of the material, labeled  $m$  in the previous equation, the value  $m = 3.5$  was used for evaluating the shaft loads and  $m = 10$  for the blade loads, since these are typical values for steel and composite materials, respectively.

The top figure reports results obtained with the B-IPC controller, while the bottom one with the proposed multi-layer controller; in both cases, comparisons are made with respect to the use of the sole collective PID trimmer.

These plots show significant reductions slightly larger than 40% in both STD and DEL for the goal quantity, i.e. the shaft bending moment. The HHC layer brings some further improvement to the performance of the B-IPC controller, pushing the load reduction to slightly above 45%. In terms of blade loads, the new scheme and B-IPC show very similar behavior. In all cases, the effects on power are quite small, with only a marginal rise in power STD, and this remains true for any mean wind speed in the full load region.

A more complete view of the performance gain in terms of shaft DEL is given by Fig. 7. For some wind speeds between the cut-in and cut-out speed values, this plot shows a comparison between the percent reduction of the shaft bending DEL obtained with B-IPC and with the multi-layer controller. In both cases, percent reductions are computed with respect to the performance of the trimmer. The figure shows that the HHC loop improves of a few percent points the performance of B-IPC, especially close to the cut-in and cut-out wind speeds. The improvement in region II is noteworthy, because here the demanded pitch command is often limited by a physical constraint on minimum pitch. On the other hand, there is little difference between the two approaches in the transition between regions II and III.

Finally, Fig. 8 gives a comparison of various performance indices weighed with a Weibull distribution centered at 8.5 m/s. The top part of the figure shows results obtained comparing B-IPC with the trimmer, while the bottom part compares the proposed multi-layer controller with the trimmer. It appears that the addition of the higher harmonic loop leads to an overall additional decrease in shaft DEL and STD of about 5 percent points. From this point of view, the bulk of the reduction with respect to the collective control case can be attributed to the single 1P control harmonic, with only a rather more modest contribution due to the higher ones.

One should also contrast this result with the already discussed Fig. 5, which showed dramatic improvements due to the control operating at the higher harmonics in the non-turbulent wind case. In fact, one can conclude that the efficacy of higher harmonic control depends to a large extent on the intensity level of turbulence: for null or low turbulence intensity, HHC is very effective and practically quenches all target harmonics, while for higher turbulence the bulk of the load reducing effects comes from the 1P control provided by B-IPC. For intermediate levels of turbulence intensity, HHC provides for performance improvements that vary between these two extremes. Hence, it appears that HHC control might be more amenable to sites with low turbulence, and probably limited to a 5 percent improvement to higher turbulence sites.

### 3.3 Decentralized Implementation

#### 3.3.1 Load Reduction in Deterministic Wind

Next, we evaluate the performance of a decentralized implementation. In this case the target load of the HHC controller is chosen to be the total root bending moment of each blade. HHC

models at different trim points in region III were synthesized using the 1P and 2P harmonics of both inputs and outputs.

For a constant-in-time wind speed of 15 m/s and a shear layer exponent of 0.2, Fig. 9 shows the spectra of the normalized blade root bending moments. The figure clearly shows that the HHC loop drastically reduces the first two load harmonics; the third harmonic, not having been included in the control goals, is essentially unmodified.

### 3.3.2 Load Reduction in Turbulent Wind

Tests were carried out on the decentralized implementation using the same turbulent conditions described for the centralized case. Figure 10 shows a bar diagram of the results for a mean hub wind of 21 m/s, reporting percent changes in blade root and shaft bending moment STD and DEL, and STD and mean value of generated power. Here the comparison is between the collective PID trimmer and the proposed multi-layer controller, featuring a PID trimmer with decentralized HHC and external PD feedback loops, as shown in Fig. 2.

The results of Fig. 10 should be compared with those of the top part of Fig. 6. It appears that the proposed implementation gives some improvement on the blade loads when compared to B-IPC. This can be explained by reasoning that, with the proposed approach, the control targets are indeed the blade loads, while in the B-IPC formulation the controller is designed so as to reduce the fixed system loads. While reduced fixed system loads imply reduced blade loads, it appears that larger reductions are possible when the controller is specifically optimized for targeting blade loads.

The same figure also shows that, since there is no coordination among the blades in the decentralized case, the fixed system loads are reduced to a lesser extent than in the centralized or B-IPC cases. This highlights once again the fact that, if one desires a reduction in the fixed system loads, then a centralized implementation should be used; on the other hand, if one seeks a reduction in the blade loads, then a decentralized implementation should be preferred.

Here again, the output power performance is virtually unaffected.

## 4 Conclusions

In this work we have described a multi-layer architecture for the control of wind turbines. The proposed approach uses distinct control layers to target different control goals, to reflect the multi-objective nature of the problem. Three main goals have been identified here, and this has led to a three-layer architecture:

- The first goal is the trimming around a set point and the load alleviation for gusts characterized by large spatial scales, for which purposes effective controllers can be designed using collective-pitch/torque inputs with a variety of methods.
- The second goal is the reduction of slowly varying deterministic loads, for which purpose the HHC approach developed by the rotorcraft community seems to be well suited.
- The third goal is the reduction of non-deterministic loads due to small scale spatial and temporal turbulent fluctuations in the wind, for which an individual blade controller with quick reaction times is needed.

It was shown that the present algorithm can be implemented in two markedly different ways: using a decentralized architecture when the aim is the reduction of the blade loads, or using a centralized architecture when the aim is the reduction of the loads in the fixed system. In both

cases, the proposed procedures lead to a marked improvement of the performance obtained with the collective controller.

The more interesting results of the present investigation appear to be those obtained with the centralized implementation, especially since fatigue is usually one of the design drivers for components in the fixed system. In that case, the addition of the HHC loop is capable of broadening the band of affected loads with respect to the sole use of the B-IPC controller, which was used here as a benchmark for comparison. In deterministic winds, the HHC controller is capable of drastic reductions of the target harmonics, which are often completely wiped out. On the other hand, at high turbulence intensity levels the benefits of the HHC controller are less apparent, since loads are dominated by fast scales which are not captured by the HHC loop, and a good part of the load reductions with respect to the sole collective pitch case are due to the B-IPC non-deterministic loop. In between null and high turbulence, there is a continuous gradation of these effects, with excellent load reductions for the HHC at low turbulence, that progressively decrease, but never disappear completely, as the turbulence intensity increases. Space limitations have precluded the presentation of other simulation studies that were conducted on different multi-MW machines, but that were found to be completely in line with the results shown here.

Future efforts should concentrate on the field testing of the proposed approach and on its further methodological refinement. One area that is worth investigating is the possible use of on-line identification, in contrast to the off-line identification used here. In fact with on-line identification, which is performed as the machine is in operation, the model has in principle the ability to self adapt so as to reflect specific characteristics of each wind turbine (e.g., due to site specific interactions with the orography of the terrain, or other effects), or self adjust to modifications in the operating conditions (e.g., due to changes in the wind shear layer, or other effects).

## References

- [1] Bossanyi E. Individual Blade Pitch Control for Load Reduction. *Wind Energy* 2003, **6**:1919–1928.
- [2] Bossanyi E. Wind Turbine Control for Load Reduction. *Wind Energy* 2003, **6**:229–244.
- [3] Bossanyi E. Developments in Individual Blade Pitch Control. The Science of Making Torque from Wind Conference, Delft, The Netherlands, 19–21 April, 2004.
- [4] Bossanyi E. Further Load Reductions with Individual Pitch Control. *Wind Energy* 2005, **8**:481–485.
- [5] van Engelen, TG. Design Model and Load Reduction Assessment for Multi-Rotational Mode Individual Pitch Control (Higher Harmonics Control). ECN-RX–06-068. 2006 European Wind Energy Conference (EWEC 2006), Athens, Greece, 27 February–1 March, 2006.
- [6] Kanev S, van Engelen TG. Exploring the Limits in Individual Pitch Control. 2009 European Wind Energy Conference (EWEC 2009), Marseille, France, 16–19 March, 2009.
- [7] Geyler M, Caselitz P. Individual Blade Pitch Control Design for Load Reduction on Large Wind Turbines. 2007 European Wind Energy Conference (EWEC 2007), Milano, Italy, 7–10 May, 2007.

- 
- [8] Leithead WE, Neilson V, Dominguez S. Alleviation of Unbalanced Rotor Loads by Single Blade Controllers. 2009 European Wind Energy Conference (EWEC 2009), Marseille, France, 16–19 March, 2009.
- [9] Stol KA. Disturbance Tracking Control and Blade Load Mitigation for Variable-Speed Wind Turbines'. *ASME Journal of Solar Energy Engineering* 2003, **125**:396–401.
- [10] Bottasso CL, Croce A. *Power Curve Tracking with Tip Speed Constraint using LQR Regulators*. Scientific Report DIA-SR 09-04, Dipartimento di Ingegneria Aerospaziale, Politecnico di Milano, March 2009.
- [11] Bottasso CL, Croce A. *Advanced Control Laws for Variable-Speed Wind Turbines and Supporting Enabling Technologies*. Scientific Report DIA-SR 09-01, Dipartimento di Ingegneria Aerospaziale, Politecnico di Milano, Milano, Italy, January 2009.
- [12] Johnson W. *Self-Tuning Regulators for Multicyclic Control of Helicopter Vibration*. NASA Technical Paper, Ames Research Center, Moffett Field, CA, USA, 1996.
- [13] Nguyen K, Betzina M, Kitaplioglu C. *Full-Scale Demonstration of Higher Harmonic Control for Noise and Vibration Reduction on the XV-15 Rotor*. Army/NASA Rotorcraft Division, NASA Ames Research Center, Moffett Field, CA, USA, 2000.
- [14] Patt D, Liu L, Chandrasekar J, Bernstein DS, Friedmann PP. Higher-Harmonic-Control Algorithm for Helicopter Vibration Reduction Revisited. *Journal of Guidance, Control and Dynamics* 2005, **28**:918–930.
- [15] Lovera M, Colaneri P, Malpica C, Celi R. Discrete-Time, Closed-Loop Aeromechanical Stability Analysis of Helicopters with Higher Harmonic Control. *Journal of Guidance, Control and Dynamics* 2007, **30**:1249–1260.
- [16] Johnson W. *Helicopter Theory*. Princeton University Press, Princeton, NJ, 1981.
- [17] Bauchau OA, Bottasso CL, Nikishkov YG. Modeling Rotorcraft Dynamics with Finite Element Multibody Procedures. *Mathematics and Computer Modeling* 2001, **33**:1113–1137.

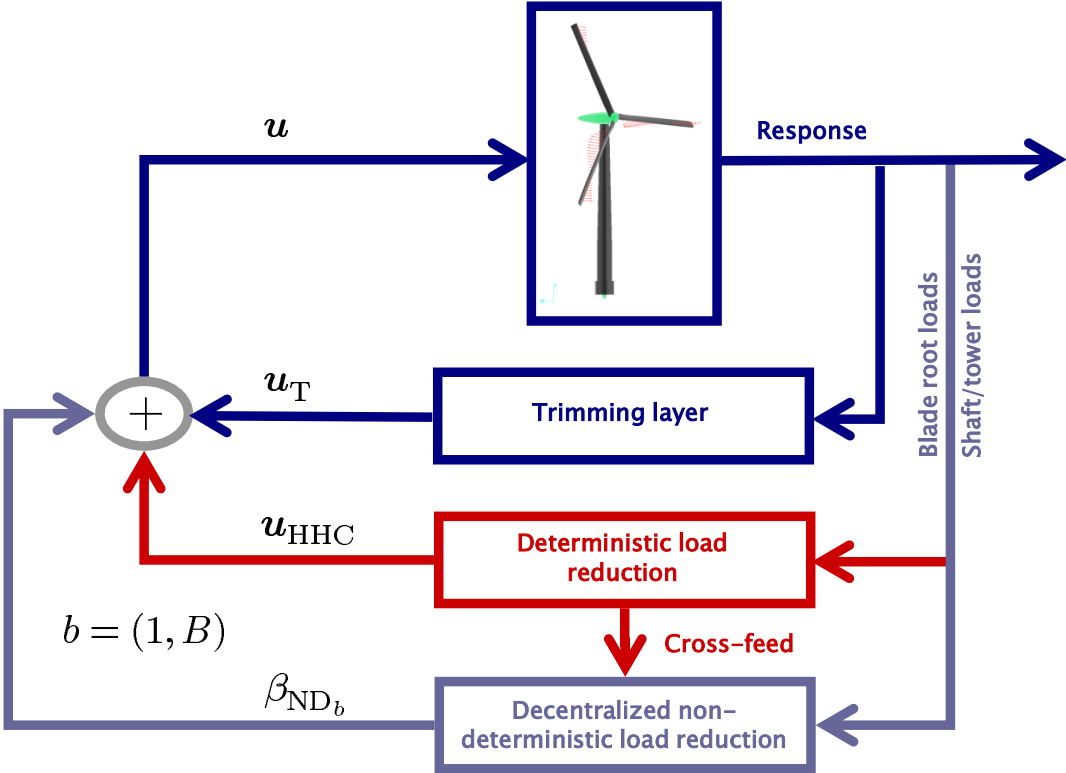


Fig. 1: Control architecture. Inner loop: centralized trimmer; middle loop: deterministic load reduction; outer loop: non-deterministic load reduction.

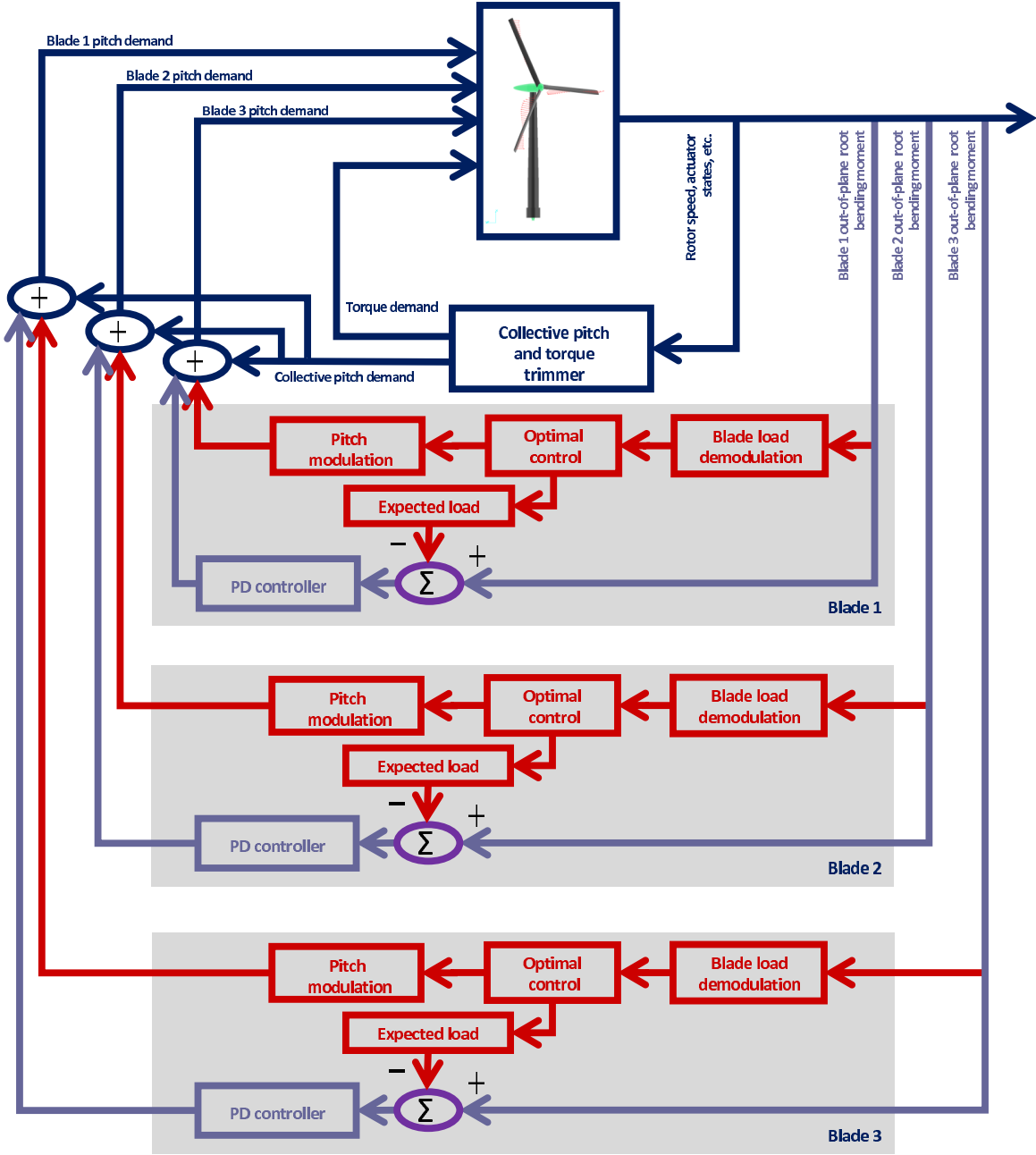


Fig. 2: Decentralized control architecture.

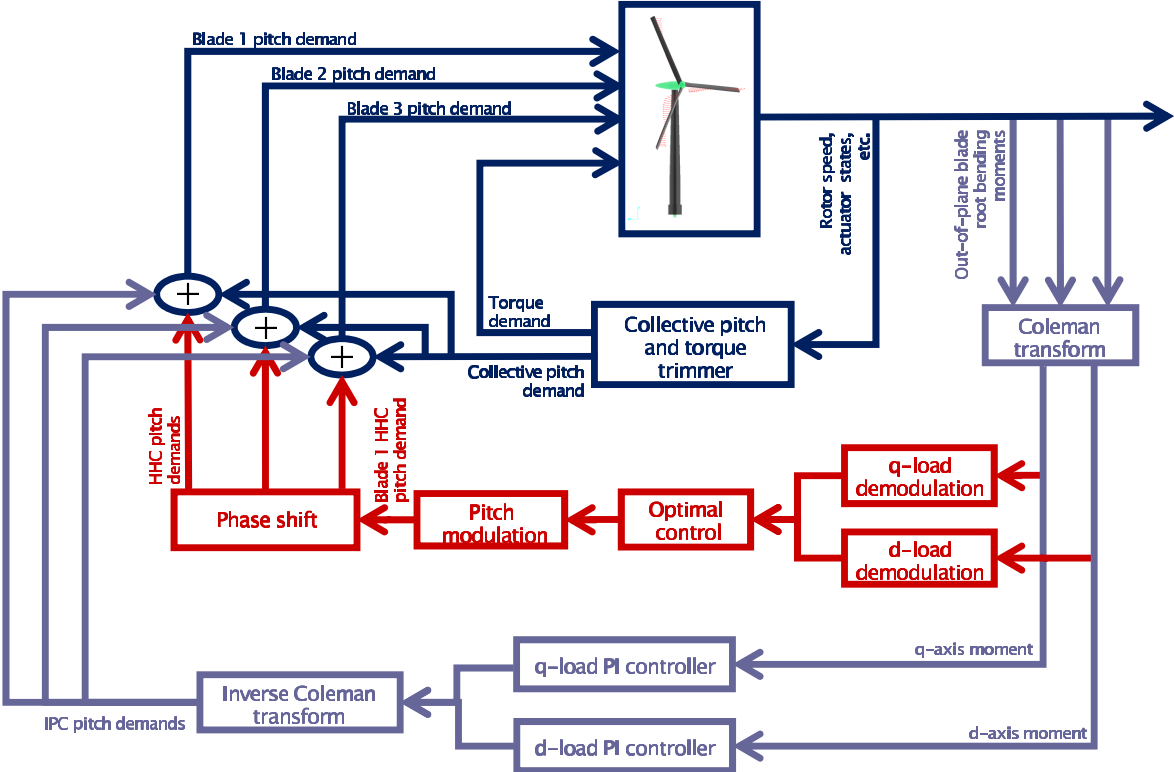


Fig. 3: Centralized control architecture.

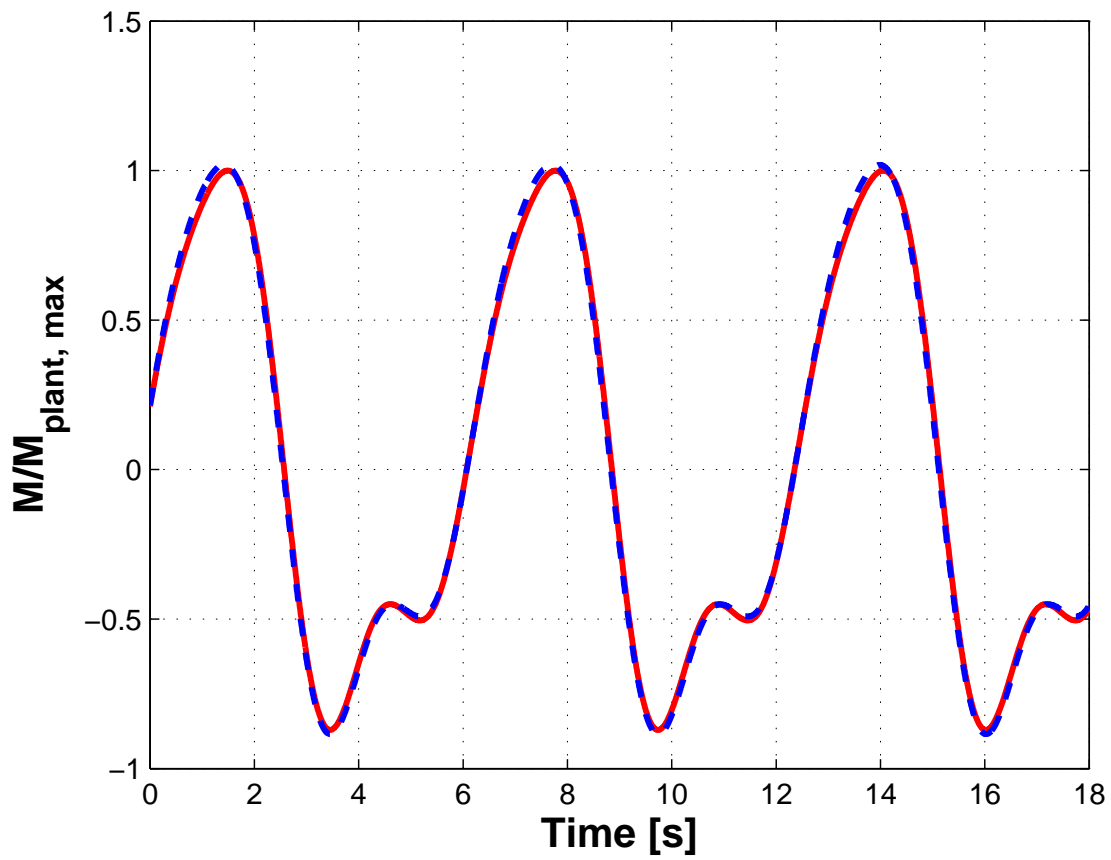


Fig. 4: Comparison between plant and identified model outputs (bade out-of-plane bending moment) for a same excitation, for a trim point at  $V=19$  m/s. Multibody plant: solid line; identified model: dashed line.

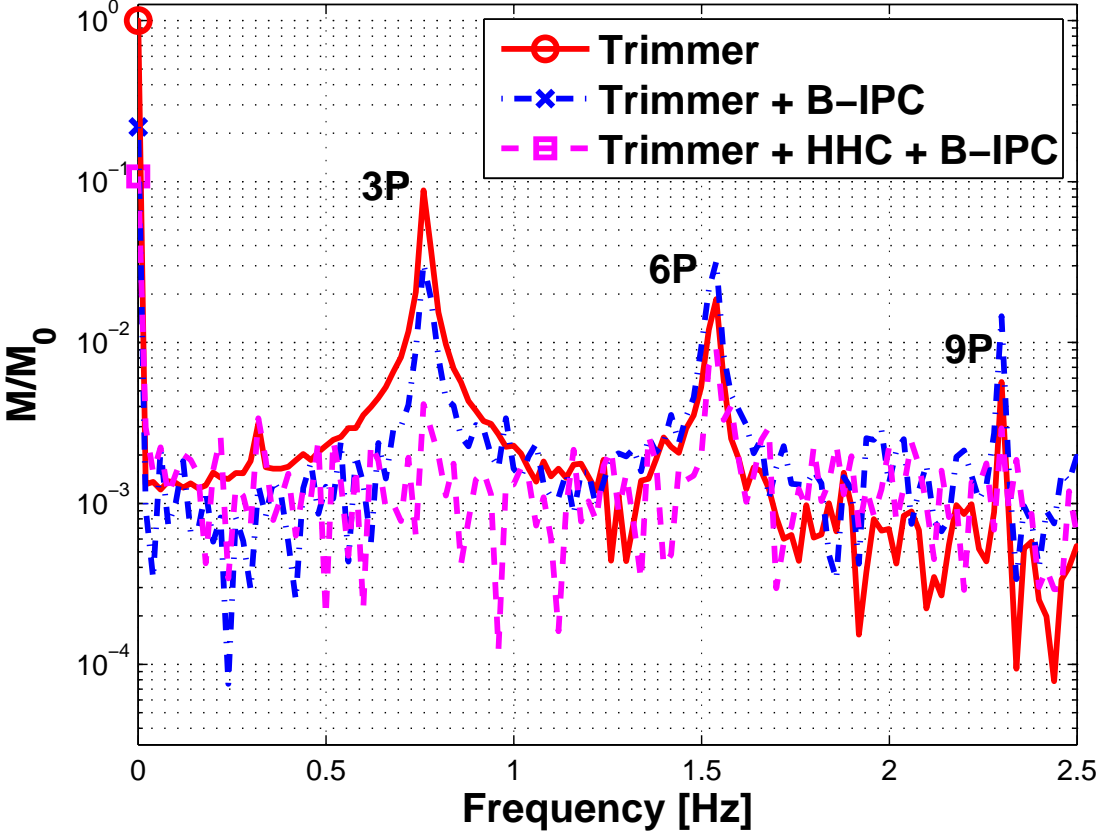


Fig. 5: Reduction of shaft bending moment resultant in deterministic wind at  $V=15$  m/s for different control systems. The spectra are normalized to the zero-frequency peak value obtained with the sole collective trimmer.

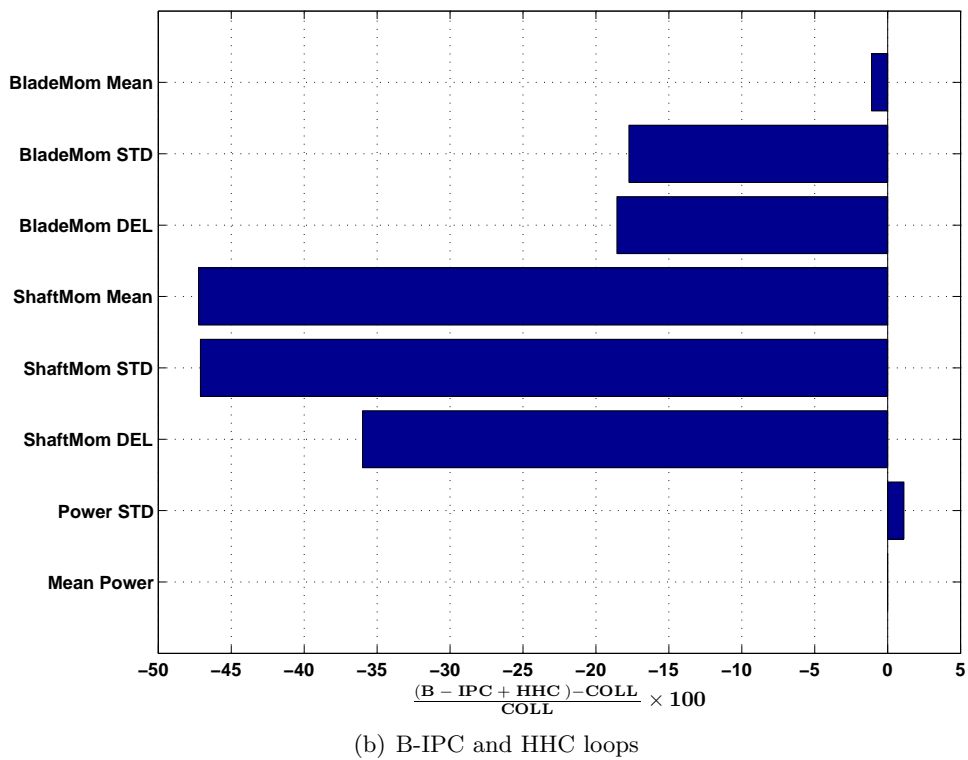
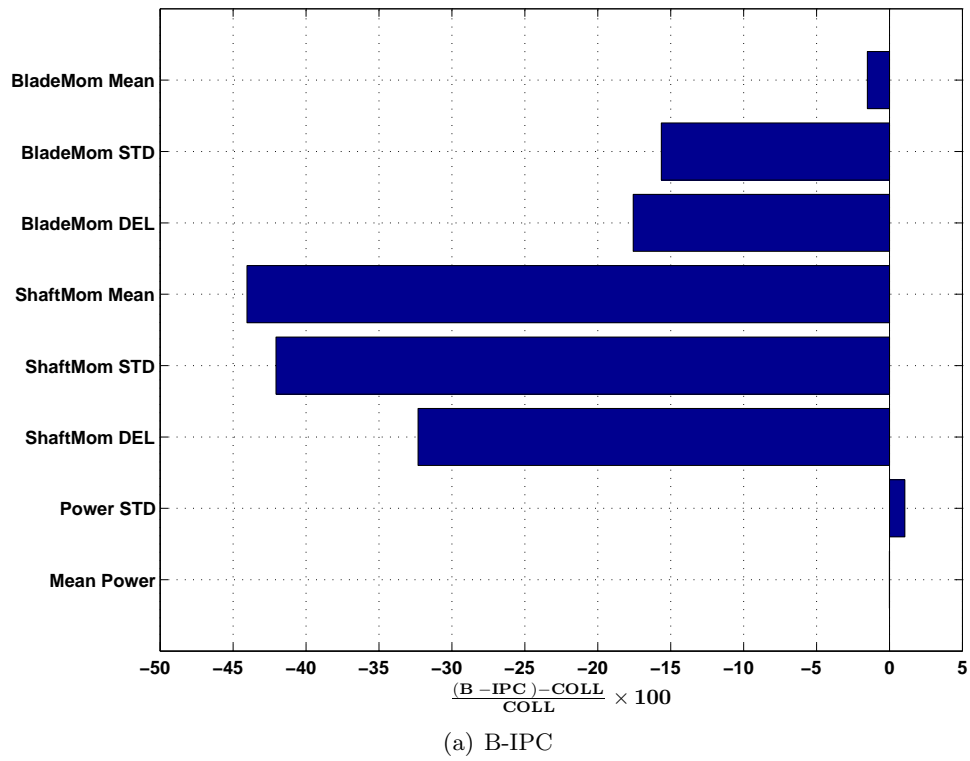


Fig. 6: Percent differences (wrt collective PID trimmer) of some physical quantities for operation in turbulent wind at  $V=21$  m/s mean speed. Top: collective PID trimmer with B-IPC. Bottom: collective PID trimmer with centralized HHC and external B-IPC loops.

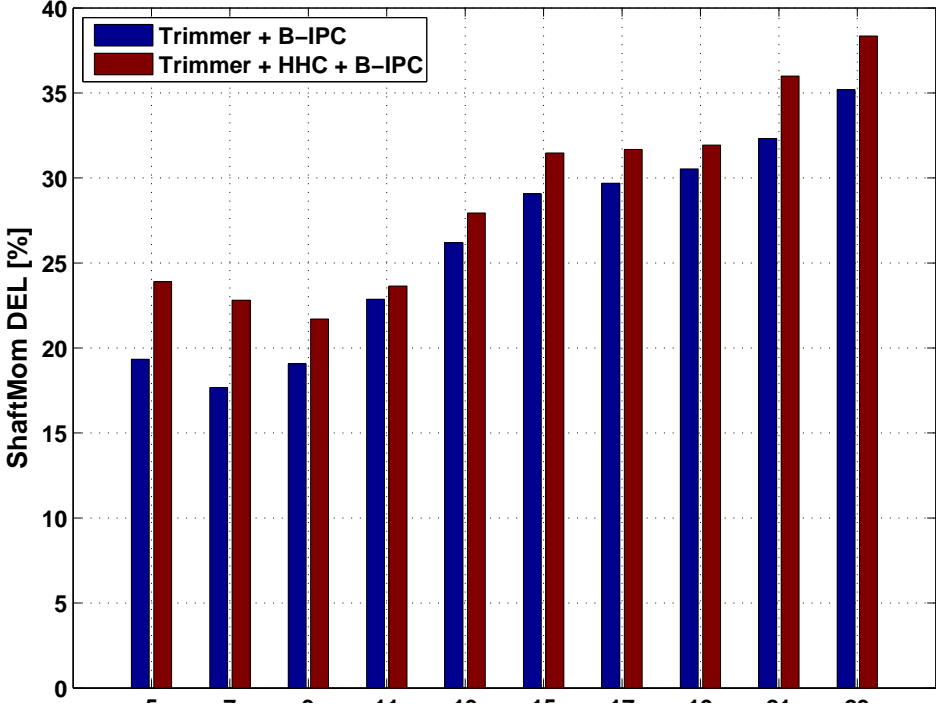
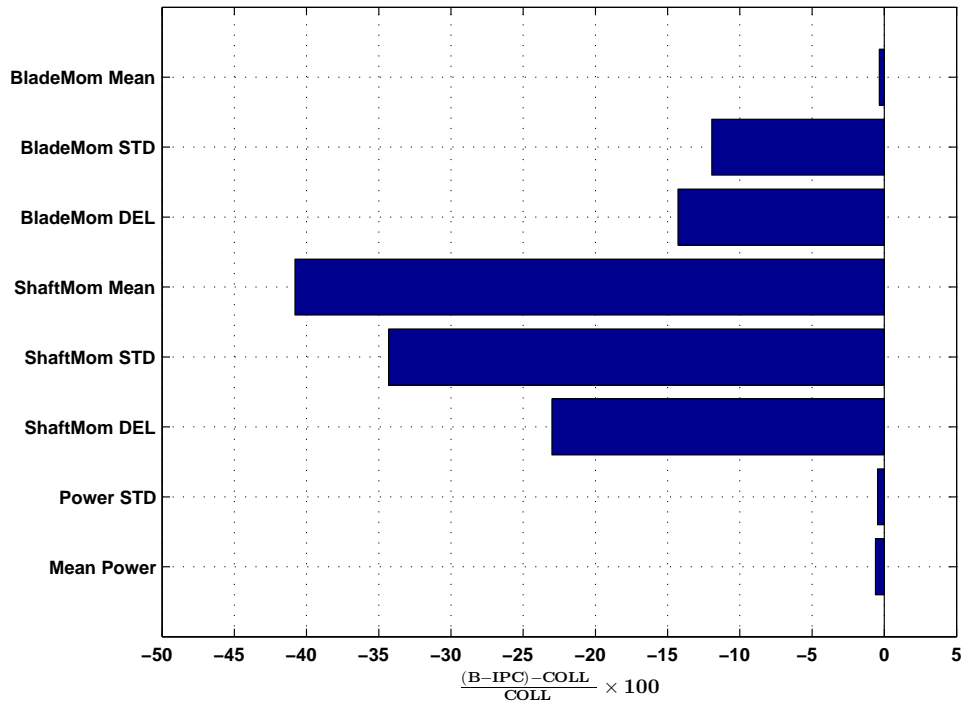
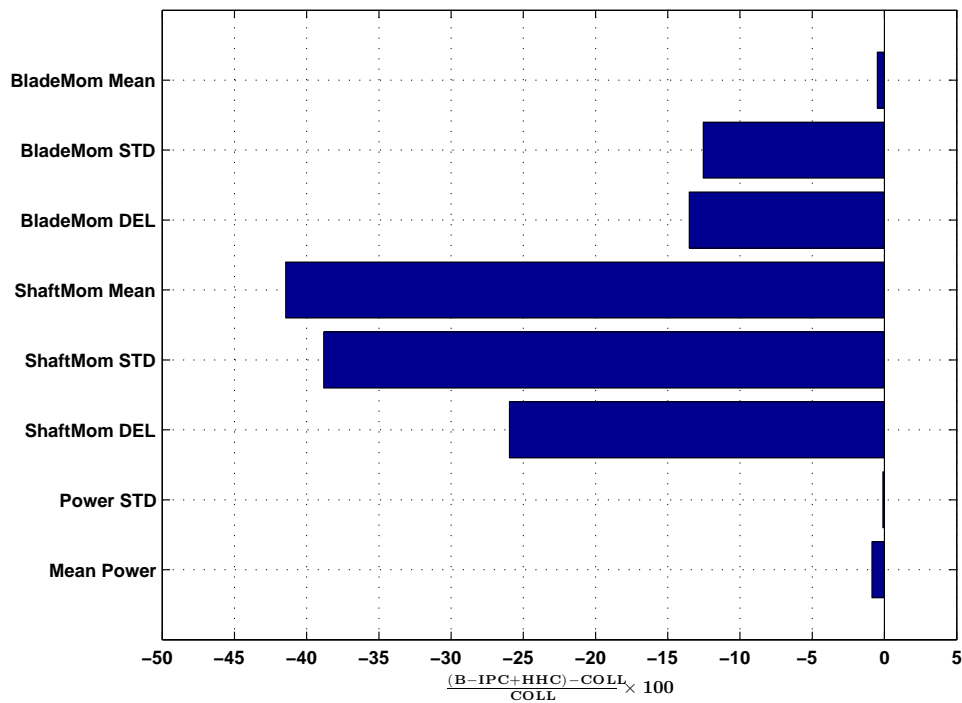


Fig. 7: Percent performance gains (wrt collective PID trimmer) on shaft bending moment DEL for operation in turbulent wind at several wind speeds between cut-in and cut-out, using collective PID trimmer with B-IPC (left columns) or PID trimmer with B-IPC and HHC loops (right columns). Positive gain values correspond to a load reduction with respect to the trimmer.



(a) B-IPC



(b) B-IPC and HHC loops

Fig. 8: Percent differences (wrt collective PID trimmer) of some physical quantities for operation in turbulent wind, weighed with a Weibull distribution centered at 8.5 m/s. Top: collective PID trimmer with B-IPC. Bottom: collective PID trimmer with centralized HHC and external B-IPC loops.

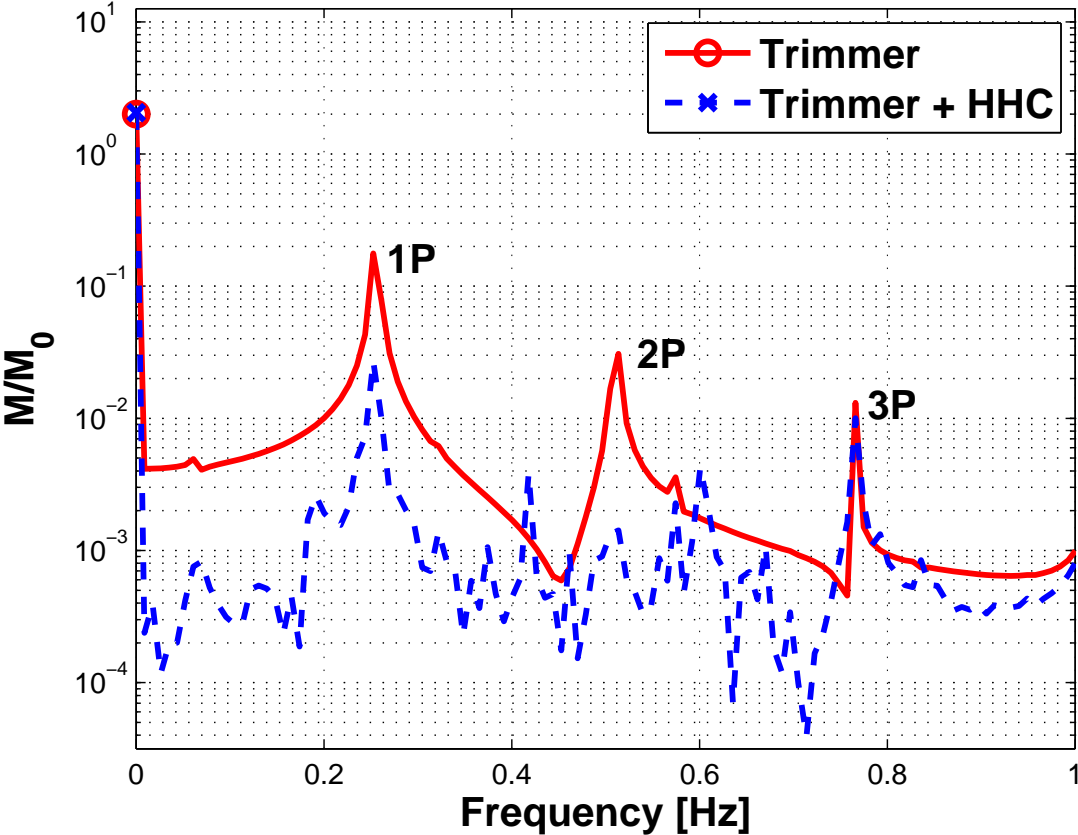


Fig. 9: Blade load reduction in deterministic wind at  $V=15$  m/s for different control systems. The spectra are normalized to the zero-frequency peak value obtained with the sole collective trimmer.

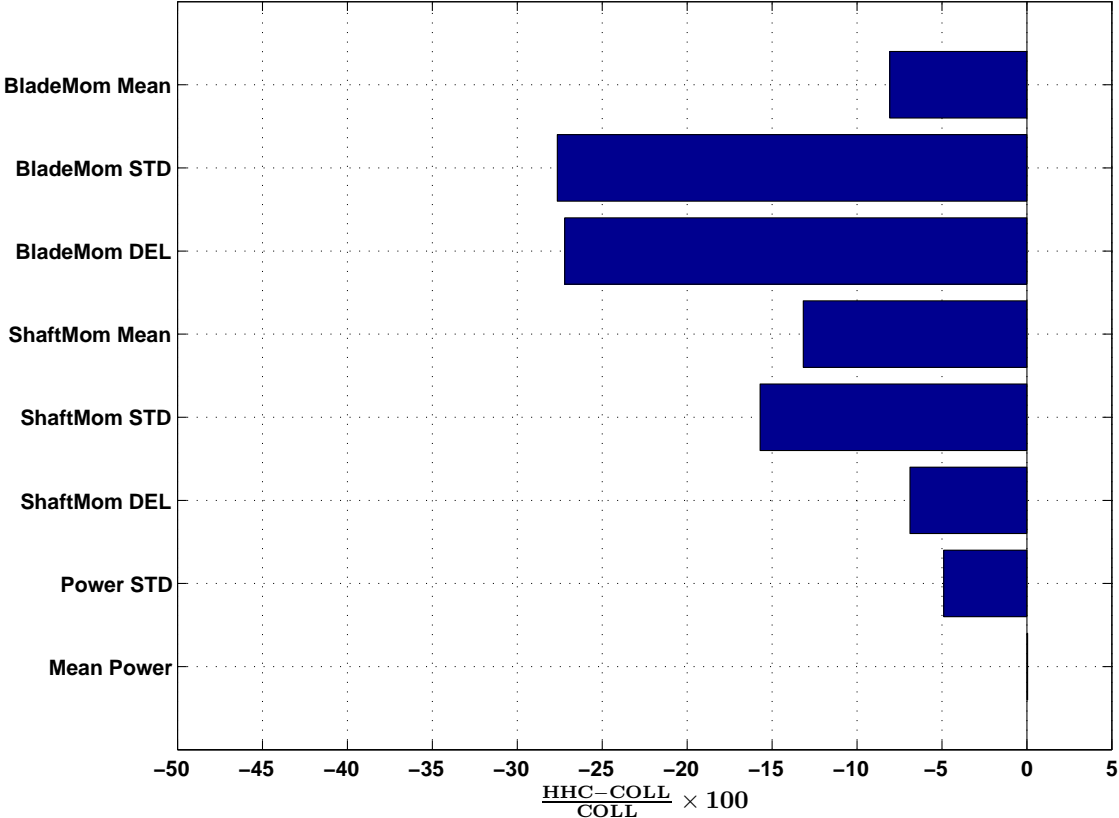


Fig. 10: Percent differences (wrt collective PID trimmer) of some physical quantities for operation in turbulent wind at V=21 m/s mean speed, using a collective PID trimmer with decentralized HHC and external PD loops.